Inorg. Chem. **2009**, *48*, 2407−2419

Influence of Alkoxyl Substituent on 4,6-Diphenyl-2,2′-bipyridine Ligand on Photophysics of Cyclometalated Platinum(II) Complexes: Admixing Intraligand Charge Transfer Character in Low-Lying Excited States

Pin Shao,[†] Yunjing Li,[†] Alexander Azenkeng,[‡] Mark R. Hoffmann,[§] and Wenfang Sun*,[†]

Department of Chemistry and Molecular Biology, North Dakota State University, Fargo, North Dakota 58105-5516, Energy and Environmental Research Center, University of North Dakota, Grand Forks, North Dakota 58202-9018, and Department of Chemistry, University of North Dakota, Grand Forks, North Dakota 58202-9024

Received August 20, 2008

A series of platinum 4,6-diphenyl-2,2′-bipyridine complexes (**6**−**10**) with alkoxyl substituent on the 6-phenyl ring have been synthesized and characterized. The influence of the alkoxyl substituent on the nature of the low-lying excited states, and thus the photophysical properties, have been systematically investigated spectroscopically and theoretically. Complexes **6**−**10** exhibit a broad low-energy charge-transfer absorption band from 400 to 500 nm, which shows weak negative solvatochromic effect. They all emit at about 590 nm in fluid solutions at room temperature, with the emission energy essentially independent of the nature of the monodentate ligand and the polarity of solvent. The excited-state lifetimes of **6** and **7** are much longer (∼460−570 ns) than those of their corresponding "alkoxyl free" analogues **12** and **13** (∼40−100 ns) in CH_3CN. Additionally, the emission quantum yields of **7**−**9** in CH_2Cl_2 are quite high (0.15−0.21). Spectroscopic studies and Time-Dependent Density Functional Theory (TDDFT) calculations indicate that these unique photophysical properties are induced by the electron-donating ability of the alkoxyl substituent, which causes a mixture of the intraligand charge transfer (ILCT) with the metal-to-ligand charge transfer (MLCT)/ligand-to-ligand charge transfer (LLCT) in their low-lying excited states. Complexes **6**−**10** exhibit broad triplet transient difference absorption in the near-UV to the near-IR region, where reverse saturable absorption (RSA) could occur. Nonlinear absorption experiments at 532 nm for nanosecond laser pulses demonstrate that **6**−**9** are strong reverse saturable absorbers, while **10** exhibits weak RSA because of its larger ground-state absorption cross-section and its low triplet excited-state quantum yield.

Introduction

In recent years, a variety of platinum(II) complexes with polypyridine ligands have been synthesized, and their spectroscopic properties have been extensively studied.[1−9] The square-planar configuration of these complexes could facilitate electron delocalization and thus lead to various intramolecular charge transfers, such as metal-to-ligand charge transfer (MLCT), ligand-to-ligand charge transfer (LLCT), or intraligand charge transfer (ILCT). This character is usually reflected in the low-energy absorption band of their UV−vis absorption spectra and in their emission spectra. The versatile spectroscopic properties of these complexes

* To whom correspondence should be addressed. E-mail: wenfang.sun@ndsu.edu.
[†] North Dakota State University.
[‡] Energy and Environmental Research Center, University of North Dakota.
[§] Department of Chemistry, University of North Dakota.

(1) Eryazici, I.; Moorefield, C. N.; Newkome, G. R. *Chem. Rev.* **2008**, *108*, 1834.
(2) (a) Lu, W.; Mi, B. X.; Chan, M. C. W.; Hui, Z.; Che, C. M.; Zhu, N.; Lee, S. T. *J. Am. Chem. Soc.* **2004**, *126*, 4958. (b) Yesin, H.; Donges, D.; Humbs, W.; Strasser, J.; Sitters, R.; Glasbeek, M. *Inorg. Chem.* **2002**, *41*, 4915. (c) Brooks, J.; Babayan, Y.; Lamansky, S.; Djurovich, P. I.; Tsyba, I.; Bau, R.; Thompson, M. E. *Inorg. Chem.* **2002**, *41*, 3055. (d) Shi, J. C.; Chao, H. Y.; Fu, W. F.; Peng, S. M.; Che, C. M. *J. Chem. Soc., Dalton Trans.* **2000**, *18*, 3128. (e) Maestri, M.; Sandrini, D.; Balzani, V.; Chassot, L.; Jolliet, P.; von Zelewsky, A. *Chem. Phys. Lett.* **1985**, *122*, 375. (f) Wong, W.-Y.; He, Z.; So, S.-K.; Tong, K.-L.; Lin, Z. *Organometallics* **2005**, *24*, 4079.
(3) (a) Islam, A.; Sugihara, H.; Hara, K.; Singh, L. P.; Katoh, R.; Yanagida, M.; Takahashi, Y.; Murata, S.; Arakawa, H. *Inorg. Chem.* **2001**, *40*, 5371. (b) Chakraborty, S.; Wadas, T. J.; Hester, H.; Flaschenreim, C.; Schmehl, R.; Eisenberg, R. *Inorg. Chem.* **2005**, *44*, 6284. (c) Geary, E. A. M.; Yellowlees, L. J.; Jack, L. A.; Oswald, I. D. H.; Parsons, S.; Hirata, N.; Durrant, J. R.; Robertson, N. *Inorg. Chem.* **2005**, *44*, 242.

10.1021/ic801589q CCC: $40.75
Published on Web 02/18/2009

enable their potential applications in organic light-emitting devices,[2] dye-sensitized solar cells,[3] photocatalysis,[4] biosensors,[5] and nonlinear optical materials.[6]

In general, the lowest-energy excited states play an important role in the photophysical properties of the complexes, such as the absorption/emission spectra, emission quantum yields, lifetimes, and transient difference absorption (TA). As reported in the literature for most of the platinum(II) terpyridyl complexes, the low-lying absorption band in the UV−vis absorption spectrum mainly arises from the metal-to-ligand charge transfer (MLCT) transition, possibly mixed with some LLCT character in case of the presence of an acetylide ancillary ligand.[1,7a,10] In these transitions, the lowest unoccupied molecular orbital (LUMO) has predominant contribution from the terpyridyl ligand, while the highest occupied molecular orbital (HOMO) is dominated by the platinum d-orbital in the case of MLCT transition and/or centered on the alkynyl ligand for the LLCT transition. Therefore, structural modification is pivotal for tuning the excited-state properties. Our previous studies on the nonlinear absorption of the platinum(II) terdentate complexes have demonstrated that the excited-state characteristics of the complexes directly affect their nonlinear absorption properties.[6] The broadest and strongest nonlinear absorption observed so far arises from the platinum(II) 4,6-diphenyl-2,2′-bipyridine complex.[6f] However, because of the very small ground-state absorption cross-sections above 550 nm for this complex, it is very difficult to sufficiently populate the excited state unless very high concentration solutions are used. Unfortunately, the solubility of this complex in common organic solvents is limited, which prevents its potential application in photonic devices that require appreciable ground-state absorption. To solve this problem, it is extremely important to increase the solubility of this complex while maintaining its broad and strong excited-state absorption. To realize this goal, a branched alkoxyl substituent is proposed to be incorporated on the 6-phenyl ring. It is expected that the alkoxyl substituent would reduce the intermolecular π,π stacking and therefore increase the solubility. Moreover, the electron-donating ability of the alkoxyl substituent could increase the electron density on the 6-phenyl ring where it is attached, which would in turn influence the lowest-energy excited-state characteristics and thus alter the nonlinear absorption of the resultant complexes.

Scheme 1 displays the synthetic procedures and the structures of the target complexes. Five monodentate ligands with different π-electron systems (except for chloride ligand) were used in these complexes to investigate the electronic effect of the ancillary ligand. All these new platinum complexes were fully characterized, and their photophysical properties and nonlinear absorption were systematically investigated. To understand the effect of the alkoxyl substituent on photophysical properties of **5**−**10**, photophysics of their corresponding "alkoxyl free" analogues **11**, **12** and **13** (Chart 1) were also investigated. In addition, Density Functional Theory (DFT) calculations were carried out on **6**−**8** and **12** with the aim to characterize the highest few occupied and lowest few unoccupied molecular orbitals, and Time-Dependent (TD) DFT calculations were performed to understand the natures of the low-lying excited states, and to verify and elucidate the observed photophysical characteristics.

Experimental Section

Synthesis. Precursors **1**, **2** and $Pt(DMSO)_2Cl_2$ were synthesized following the literature procedures.[11] The synthesis of **11**−**13** were reported previously.[6f,12] All the other chemicals and solvents were purchased from Alfa Aesar and used as is unless otherwise stated. Column chromatography was carried out using silica gel (Sorbent Technologies, 60 Å, 230 × 450 mesh) or neutral aluminum oxide (Sigma-Aldrich, 58 Å, ∼150 mesh).

^{1}H NMR spectra were measured on a Varian 300 or 400 MHz VNMR spectrometer. Elemental analyses were conducted by

(4) (a) Zhang, D.; Wu, L. Z.; Zhou, L.; Han, X.; Yang, Q. Z.; Zhang, L. P.; Tung, C. H. *J. Am. Chem. Soc.* **2004**, *126*, 3440. (b) Du, P.; Schneider, J.; Jarosz, P.; Eisenberg, R. *J. Am. Chem. Soc.* **2006**, *128*, 7726. (c) Narayana-Prabhu, R.; Schmehl, R. H. *Inorg. Chem.* **2006**, *45*, 4319.

(5) Wong, K. M. C.; Tang, W. S.; Chu, B. W. K.; Zhu, N.; Yam, V. W. W. *Organometallics* **2004**, *23*, 3459.

(6) (a) Guo, F.; Sun, W.; Liu, Y.; Schanze, K. *Inorg. Chem.* **2005**, *44*, 4055. (b) Sun, W.; Wu, Z.-X.; Yang, Q.-Z.; Wu, L.-Z.; Tung, C.-H. *Appl. Phys. Lett.* **2003**, *82*, 850. (c) Sun, W.; Guo, F. *Chin. Opt. Lett.* **2005**, *S3*, S34. (d) Guo, F.; Sun, W. *J. Phys. Chem. B* **2006**, *110* (30), 15029. (e) Pritchett, T. M.; Sun, W.; Guo, F.; Zhang, B.; Ferry, M. J.; Rogers-Haley, J. E.; Shensky, W., III; Mott, A. G. *Opt. Lett.* **2008**, *33* (10), 1053. (f) Shao, P.; Li, Y.; Sun, W. *J. Phys. Chem. A.* **2008**, *112*, 1172. (g) Shao, P.; Li, Y.; Sun, W. *Organometallics* **2008**, *27*, 2743. (h) Ji, Z.; Li, Y.; Sun, W. *Inorg. Chem.* **2008**, *47*, 7599.

(7) (a) Shikhova, E.; Danilov, E. O.; Kinayyigit, S.; Pomestchenko, I. E.; Tregubov, A. D.; Camerel, F.; Retailleau, P.; Ziessel, R.; Castellano, F. N. *Inorg. Chem.* **2007**, *46*, 3038. (b) Wong, K. M.-C.; Tang, W.-S.; Lu, X.-X.; Zhu, N.; Yam, V. W.-W. *Inorg. Chem.* **2005**, *44*, 1492.

(8) (a) Michalec, J. F.; Bejune, S. A.; McMillin, D. R. *Inorg. Chem.* **2000**, *39*, 2708. (b) Ratilla, E. M. A.; Brothers, H. M., II; Kostic, N. M. *J. Am. Chem. Soc.* **1987**, *109*, 4592. (c) Yip, H. K.; Cheng, L. K.; Cheung, K. K.; Che, C. M. *J. Chem. Soc., Dalton Trans.* **1993**, 2933. (d) Michalec, J. F.; Bejune, S. A.; Cuttell, D. G.; Summerton, G. C.; Gertenbach, J. A.; Field, J. S.; Haines, R. J.; McMillin, D. R. *Inorg. Chem.* **2001**, *40*, 2193.

(9) (a) Cheung, T. C.; Cheung, K. K.; Peng, S. M.; Che, C. M. *J. Chem. Soc., Dalton Trans.* **1996**, 1645. (b) Neve, F.; Ghedini, M.; Crispini, A. *J. Chem. Soc., Chem. Commun.* **1996**, 2463. (c) Lai, S. W.; Chan, M. C. W.; Cheung, T. C.; Peng, S. M.; Che, C. M. *Inorg. Chem.* **1999**, *38*, 4046. (d) Lai, S. W.; Chan, M. C. W.; Cheung, K. K.; Che, C. M. *Organometallics* **1999**, *18*, 3327. (e) Yip, J. H. K.; Suwarno; Vittal, J. J. *Inorg. Chem.* **2000**, *39*, 3537.

(10) (a) Aldridge, T. K.; Stacey, E. M.; McMillin, D. R. *Inorg. Chem.* **1994**, *33*, 722. (b) Büchner, R; Field, J. S.; Haines, R. J.; Cunningham, C. T.; McMillin, D. R. *Inorg. Chem.* **1997**, *36*, 3952. (c) Crites, D. K.; Cunningham, C. T.; McMillin, D. R. *Inorg. Chim. Acta* **1998**, *273*, 346. (d) Büchner, R.; Cunningham, C. T.; Field, J. S.; Haines, R. J.; McMillin, D. R.; Summerton, G. C. *J. Chem. Soc., Dalton Trans.* **1999**, 711. (e) Lai, S.-W.; Chan, M. C. W.; Cheung, K.-K.; Che, C.-M. *Inorg. Chem.* **1999**, *38*, 4262. (f) Yam, V. W.-W.; Tang, R. P.-L.; Wong, K. M.-C.; Cheung, K.-K. *Organometallics* **2001**, *20*, 4476. (g) Yang, Q.-Z.; Wu, L.-Z.; Wu, Z.-X.; Zhang, L.-P.; Tung, C.-H. *Inorg. Chem.* **2002**, *41*, 5653. (h) Liu, X.-J.; Feng, J.-K.; Meng, J.; Pan, Q.-J.; Ren, A.-M.; Zhou, X.; Zhang, H.-X. *Eur. J. Inorg. Chem.* **2005**, 1856. (i) Zhou, X.; Zhang, H.-X.; Pan, Q.-J.; Xia, B.-H.; Tang, A.-C. *J. Phys. Chem. A* **2005**, *109*, 8809. (j) Hua, F.; Kinayyigit, S.; Cable, J. R.; Castellano, F. N. *Inorg. Chem.* **2006**, *45*, 4304.

(11) (a) Chang, J. Y.; Nam, S. W.; Hong, C. G.; Im, J.-H.; Kim, J.-H.; Han, M. J. *Adv. Mater.* **2001**, *13*, 1298. (b) Neve, F.; Crispini, A.; Campagna, S.; Serroni, S. *Inorg. Chem.* **1999**, *38*, 2250. (c) Price, J. H.; Williamson, A. N.; Schramm, R. F.; Wayland, B. B. *Inorg. Chem.* **1972**, *11*, 1280.

(12) Shao, P.; Sun, W. *Inorg. Chem.* **2007**, *46*, 8603.

Scheme 1. Synthetic Routes and Structures for Complexes **6**−**10**

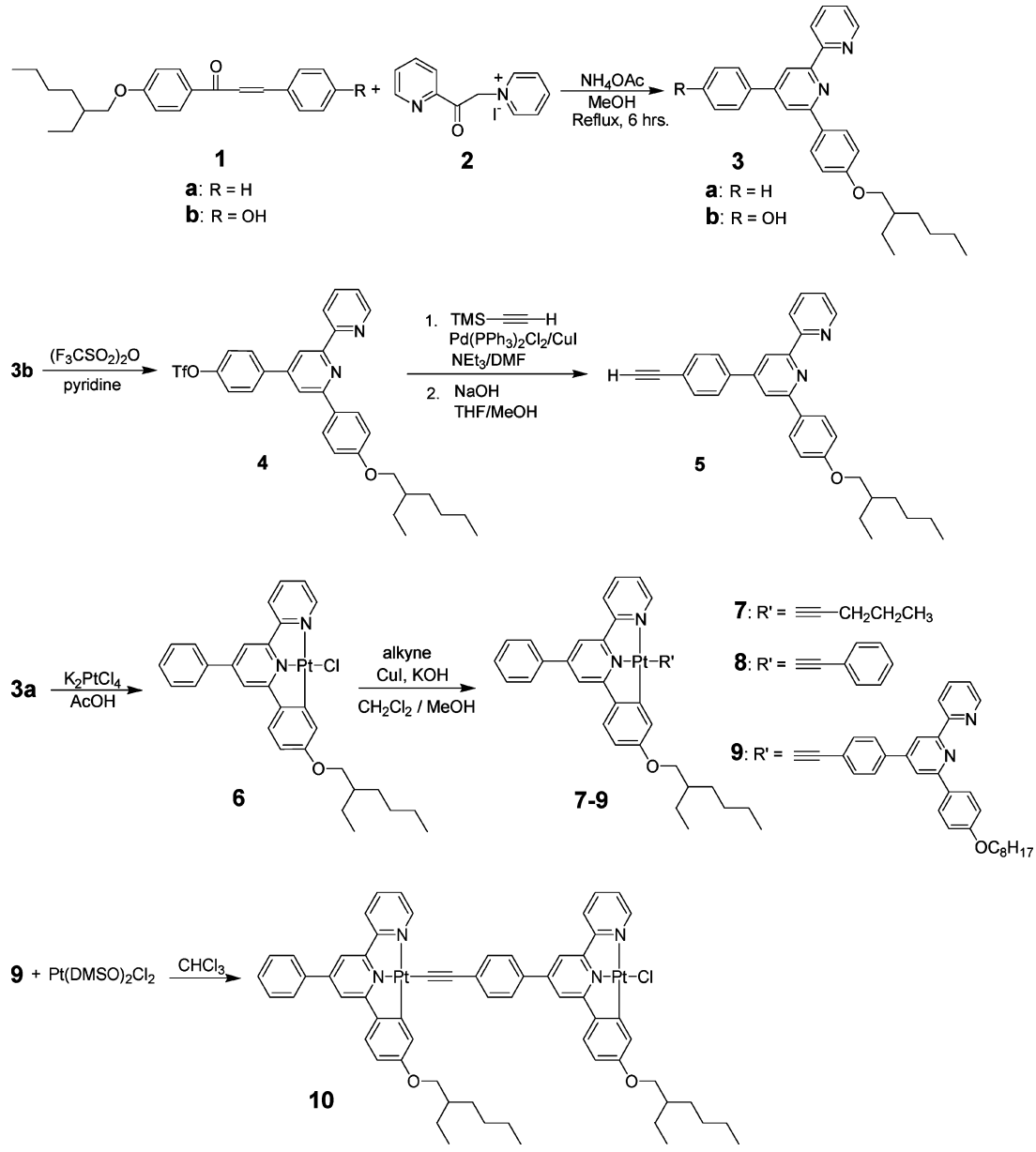

Chart 1

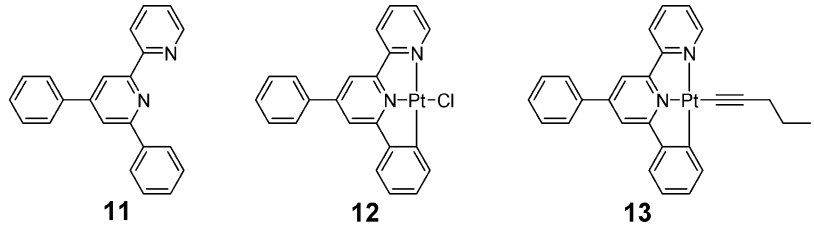

NuMega Resonance Laboratories, Inc. in San Diego, CA. ESI-HRMS analyses were conducted on a Bruker Daltonics BioTOF III mass spectrometer.

3a. A mixture of **1a** (1.24 g, 3.70 mmol), **2** (1.20 g, 3.70 mmol), and NH_4OAc (2.60 g, 37.70 mmol) in 20 mL of methanol was refluxed for 6 h. The solvent was removed under reduced pressure, and the residue was extracted with CH_2Cl_2. The CH_2Cl_2 solution was washed with water, and the solvent was then removed. The crude product was purified by passing a silica column with hexane/ethyl acetate (v/v: 20/1) used as the eluent. A 0.24 g colorless liquid was obtained (yield: 15%). ^{1}H NMR ($CDCl_3$) δ: 8.68−8.72 (m, 2H), 8.60 (d, J = 0.80 Hz, 1H), 8.16 (d, J = 8.40 Hz, 2H), 8.17 (d, J = 1.20 Hz, 1H), 7.81−7.86 (m, 3H), 7.43−7.52 (m, 3H), 7.30−7.32 (m, 1H), 7.05 (d, J = 8.80 Hz, 2H), 3.93 (d, J = 5.60 Hz, 2H), 1.75−1.81 (m, 1H), 1.28−1.63 (m, 8H), 0.88−0.99 (m, 6H).

3b. The synthetic procedure was similar to that for **3a** except **1b** instead of **1a** was used. **3b** was obtained as white solid with a yield of 69%. ^{1}H NMR ($CDCl_3$) δ: 8.74 (m, 1H), 8.68 (d, J = 7.80 Hz, 1H), 8.41 (d, J = 1.50 Hz, 1H), 8.13 (d, J = 9.00 Hz, 2H),

7.91 (td, J = 7.80 and 1.50 Hz, 1H), 7.86 (d, J = 1.50 Hz, 1H), 7.59 (d, J = 8.40 Hz, 2H), 7.39 (m, 1H), 7.04 (d, J = 9.00 Hz, 2H), 6.95 (d, J = 9.00 Hz, 2H), 6.84 (s, 1H), 3.93 (d, J = 6.00 Hz, 2H), 1.77 (m, 1H), 1.47 (m, 4H), 1.36 (m, 4H), 0.95 (t, J = 7.80 Hz, 3H).

4. 3b (2.26 g, 5.00 mmol) was dissolved in 10 mL of dry pyridine at 0 °C, and $(F_3CSO_2)_2O$ (2.10 g, 7.50 mmol) was added slowly. The mixture was stirred at 0 °C for 30 min and then at room temperature for 2 days. The resultant mixture was poured into 100 mL of ice water, and the solid was collected by filtration. The crude product was dissolved in hexane, and the undissolved solid was removed by filtration. Removal of hexane from the filtrate yielded 2.54 g of white solid (yield: 87%). ^{1}H NMR ($CDCl_3$) δ: 8.68 (m, 2H), 8.52 (s, 1H), 8.14 (d, J = 9.00 Hz, 2H), 7.84 (m, 4H), 7.40 (d, J = 9.00 Hz, 2H), 7.34 (m, 1H), 7.05 (d, J = 8.40 Hz, 2H), 3.93 (d, J = 5.70 Hz, 2H), 1.78 (m, 1H), 1.48 (m, 4H), 1.37 (m, 4H), 0.97 (t, J = 7.50 Hz, 3H).

5. A mixture of **4** (1.17 g, 2.00 mmol), $Pd(PPh_3)_2Cl_2$ (82.0 mg, 0.12 mmol), CuI (14.0 mg, 0.07 mmol), and (trimethylsily)acetylene (0.54 mL, 3.90 mmol) in 1.4 mL of freshly distilled NEt_3 and 4 mL of *N*,*N*-dimethylformamide (DMF) was stirred at 55 °C for 24 h under argon protection. After the reaction, the mixture was poured into 100 mL of water and extracted with CH_2Cl_2 three times. The CH_2Cl_2 layer was washed with brine (30 mL × 3) and dried over anhydrous $MgSO_4$. Trimethylsily protected intermediate was obtained after passing a silica column eluted with hexane/ethyl acetate (v/v: 10/1). The white intermediate (266 mg, 0.50 mmol) was dissolved in 50 mL of tetrahydrofuran (THF), and then 1.5 mL of 10% NaOH aqueous solution and 50 mL of MeOH were added. The mixture was stirred for 10 min and then neutralized with 1.0 M HCl. The organic solvents were removed, and the residue was extracted with CH_2Cl_2. The CH_2Cl_2 solution was washed with water and dried over Na_2SO_4. After removal of the solvent, 0.67 g white solid was obtained (yield: 73%). ^{1}H NMR ($CDCl_3$) δ: 8.69 (d, J = 4.40 Hz, 1H), 8.65 (d, J = 8.00 Hz, 1H), 8.55 (d, J = 1.20 Hz, 1H), 8.13 (d, J = 8.40 Hz, 2H), 7.86 (d, J = 1.20 Hz, 1H), 7.82−7.85 (m, 1H), 7.76 (d, J = 8.00 Hz, 2H), 7.61 (d, J = 8.00 Hz, 2H), 7.29−7.32 (m, 1H), 7.03 (d, J = 8.40 Hz, 2H), 3.92 (d, J = 5.60 Hz, 2H), 3.17 (s, 1H), 1.75−1.78 (m, 1H), 1.33−1.54 (m, 8H), 0.90−0.97 (m, 6H).

6. K_2PtCl_4 (0.22 g, 0.54 mmol) and ligand **3a** (0.24 g, 0.54 mmol) was refluxed in 50 mL of acetic acid for 24 h. The resultant orange solid was collected by filtration, and washed with water. The crude product was recrystalized from CH_2Cl_2/ether to obtain 0.30 g of orange solid (yield: 83%). ^{1}H NMR ($CDCl_3$) δ: 8.96 (s, 1H), 7.91−7.99 (m, 2H), 7.70 (br. s, 2H), 7.53 (d, J = 6.00 Hz, 6H), 7.38 (s, 1H), 7.16 (s, 1H), 6.58 (d, J = 11.2 Hz, 1H), 3.84 (br. s, 2H), 1.69 (br., 1H), 1.34−1.51 (m, 8H), 0.94 (t, J = 9.20 Hz, 6H). ESI-MS: m/z calcd for $[C_{30}H_{31}N_2O^{195}Pt + CH_3CN]^+$, 671.2347; found, 671.2364. Anal. Calcd for $C_{30}H_{31}ClN_2OPt$: C, 54.09; H, 4.65; N, 4.21. Found: C, 54.36; H, 4.25; N, 4.17.

7. A mixture of KOH (15.0 mg, 0.27 mmol), **6** (70.0 mg, 0.11 mmol), pentyne (15.0 μL, 0.15 mmol), and CuI (3.0 mg, 0.016 mmol) in MeOH/CH_2Cl_2 was stirred at room temperature for 24 h under argon protection. The solvent was removed under reduced pressure, and the crude product was purified by passing a short aluminum oxide column (CH_2Cl_2 was used as the eluent), and then recrystalized by diffusing ether into dilute CH_2Cl_2 solution. A 43.0 mg quantity of orange solid was obtained (yield: 56%). ^{1}H NMR ($CDCl_3$) δ: 9.17 (d, J = 5.10 Hz, 1H), 7.98 (td, J = 1.80 and 7.20 Hz, 1H), 7.90 (d, J = 7.80 Hz, 1H), 7.70 (d, J = 4.50 Hz, 1H), 7.67 (d, J = 1.50 Hz, 1H), 7.59 (d, J = 1.20 Hz, 1H), 7.56 (d, J = 2.40 Hz, 1H), 7.50−7.54 (m, 3H), 7.44−7.49 (m, 2H), 7.30 (d, J = 8.40 Hz, 1H), 6.58 (dd, J = 2.70 and 8.40 Hz, 1H), 3.94 (d, J = 6.30 Hz, 2H), 2.67 (t, J = 6.90 Hz, 2H), 1.69−1.76 (m, 3H), 1.35−1.53 (m, 8H), 1.15 (t, J = 7.20 Hz, 3H), 0.95 (t, J = 0.75 Hz, 6H). ESI-MS: m/z calcd for $[C_{35}H_{38}N_2O^{195}Pt-H]^+$, 696.2551; found, 696.2633. Anal. Calcd for $C_{35}H_{38}N_2OPt$: C, 60.25; H, 5.49; N, 4.01. Found: C, 59.95; H, 5.48; N, 4.01.

8. A mixture of phenylacetylene (15.0 μL, 0.14 mmol) and KOH (9.0 mg, 0.15 mmol) in 10 mL of MeOH and 25 mL of CH_2Cl_2 was purged with argon for 20 min, and then **6** (46.0 mg, 0.07 mmol) and CuI (3.0 mg, 0.016 mmol) were added. The mixture was stirred at room temperature for 24 h under argon protection. The solvents were removed, and the crude product was purified by aluminum oxide column with CH_2Cl_2 as the eluent. A 32.0 mg quantity of yellow solid was obtained (yield: 71%). ^{1}H NMR ($CDCl_3$) δ: 9.21 (d, J = 4.80 Hz, 1H), 8.01 (t, J = 8.00 Hz, 1H), 7.93 (d, J = 8.00 Hz, 1H), 7.67−7.69 (m, 2H), 7.62 (s, 1H), 7.49−7.57 (m, 7H), 7.33 (d, J = 8.00 Hz, 1H), 7.23−7.25 (m, 3H), 7.16 (t, J = 7.60 Hz, 1H), 6.58 (dd, J = 2.80 and 8.40 Hz, 1H), 3.91 (d, J = 6.00 Hz, 2H), 1.69−1.74 (m, 1H), 1.29−1.49 (m, 8H), 0.86−0.94 (m, 6H). ESI-MS: m/z calcd for $[C_{38}H_{36}N_2O^{195}Pt + H]^+$, 732.2552; found, 732.2557. Anal. Calcd for $C_{38}H_{36}N_2OPt$: C, 62.37; H, 4.96; N, 3.83. Found: C, 61.99; H, 4.84; N, 3.84.

9. A mixture of KOH (28.0 mg, 0.50 mmol), **6** (230.0 mg, 0.35 mmol), **5** (160.0 mg, 0.35 mmol), and CuI (3.0 mg, 0.016 mmol) in MeOH/CH_2Cl_2 was stirred at room temperature for 24 h under the protection of argon. The solvent was removed under reduced pressure, and the crude product was purified by passing a short aluminum oxide column with CH_2Cl_2 as the eluent and recrystalized by diffusing ether into dilute CH_2Cl_2 solution. A 246 mg quantity of red solid was obtained (yield: 64%). ^{1}H NMR ($CDCl_3$) δ: 9.10 (d, J = 5.00 Hz, 1H), 8.76 (dd, J = 4.50 and 1.00 Hz, 1H), 8.72 (d, J = 8.00 Hz, 1H), 8.66 (d, J = 1.00 Hz, 1H), 8.20 (d, J = 9.00 Hz, 2H), 7.99 (d, J = 1.00 Hz, 1H), 7.97 (d, J = 7.50 Hz, 1H), 7.88−7.92 (m, 2H), 7.81 (d, J = 8.00 Hz, 2H), 7.73−7.75 (m, 2H), 7.69 (d, J = 7.50 Hz, 2H), 7.61 (s, 1H), 7.51−7.52 (m, 4H), 7.45 (s, 1H), 7.42−7.44 (m, 1H), 7.35−7.38 (m, 1H), 7.30 (s, 1H), 7.08 (d, J = 8.50 Hz, 2H), 6.60 (dd, J = 2.50 and 8.50 Hz, 1H), 3.97 (d, J = 6.00 Hz, 2H), 3.92 (d, J = 5.50 Hz, 2H), 1.77−1.82 (m, 2H), 1.37−1.60 (m, 16H), 0.92−1.01 (m, 12H). ESI-MS: m/z calcd for $[C_{62}H_{62}N_4O_2{}^{195}Pt + H]^+$, 1090.4598; found, 1090.4568. Anal. Calcd for $C_{62}H_{62}N_4O_2Pt$: C, 68.30; H, 5.73; N, 5.14. Found: C, 68.31; H, 6.12; N, 5.32.

10. A mixture of **9** (170.0 mg, 0.16 mmol) and $Pt(DMSO)_2Cl_2$ (68.0 mg, 0.16 mmol) in 15 mL of $CHCl_3$ was refluxed for 24 h. The solvent was removed by rotator evaporation, and the crude product was purified by passing a short aluminum oxide column eluted with CH_2Cl_2, and then further purified by diffusing ether into dilute CH_2Cl_2 solution to yield 100 mg of a red solid (yield: 47%). ^{1}H NMR ($CDCl_3$) δ: 8.85 (br. s, 2H), 7.87−7.92 (m, 4H), 7.67 (s, 4H), 7.49 (s, 8H), 7.40 (br., 2H), 7.31 (s, 2H), 7.18 (d, J = 8.80 Hz, 2H), 7.10 (s, 1H), 6.53 (d, J = 8.40 Hz, 2H), 3.80 (br., 4H), 1.66 (m, 2H), 1.32−1.55 (m, 16H), 0.91−0.93 (m, 12H). Anal. Calcd for $C_{62}H_{61}ClN_4O_2Pt_2$: C, 56.42; H, 4.66; N, 4.25. Found: C, 56.04; H, 4.26; N, 4.30.

Photophysical Measurements. The UV−vis absorption spectra were measured using an Agilent 8453 spectrophotometer in a 1 cm or 1 mm quartz cuvette. The steady state emission spectra were obtained on a SPEX fluorolog-3 fluorometer/phosphorometer. The emission quantum yields were determined by the comparative method[13] in degassed CH_2Cl_2 and CH_3CN solutions, respectively. A degassed aqueous solution of $[Ru(bpy)_3]Cl_2$ (Φ_{em} = 0.042, λ_{ex}

(13) Demas, J. N.; Crosby, G. A. *J. Phys. Chem.* **1971**, *75*, 991.

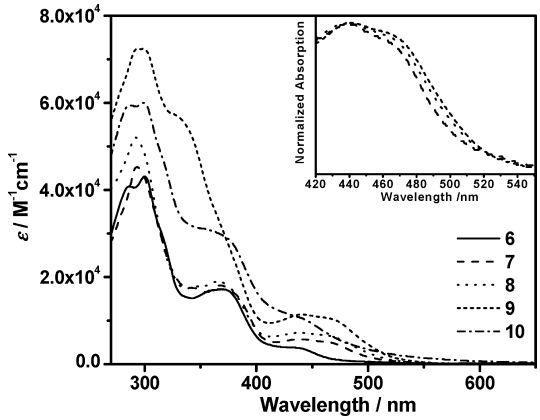

Figure 1. Electronic absorption spectra of **6**−**10** in CH_2Cl_2. The inset shows the normalized low-energy absorption band for **7**−**9**.

= 436 nm) was used as the reference.[14] The excited-state lifetimes, triplet excited-state quantum yields, and the triplet transient difference absorption spectra were measured in CH_3CN solutions on an Edinburgh LP920 laser flash photolysis spectrometer. The third harmonic output (355 nm) of a Nd:YAG laser (Quantel Brilliant, pulsewidth (fwhm) = 4.1 ns, repetition rate = 10 Hz) was used as the excitation source. Each sample was purged with Ar for 30 min before measurement.

The intrinsic excited-state lifetime (τ_0) of the complex and the emission self-quenching rate constants (k_q) in CH_2Cl_2 were obtained from the Stern−Volmer equation:

$$k_{obs} = k_q[C] + k_0 \quad (1)$$

where k_{obs} is the observed emission decay rate constants ($k_{obs} = 1/\tau_{em}$) at a given concentration, k_q is the self-quenching rate constant, [C] is the concentration of the solution, and k_0 ($k_0 = 1/\tau_0$) is the decay rate constant of the excited state at infinite dilute solution. The lifetimes of the complex in a series of solutions with different concentrations were measured. The obtained k_{obs}'s were plotted against the solution concentrations, and a straight line was obtained. The slope of the straight line corresponds to the k_q, and the intercept is the k_0.

The molar extinction coefficient of the triplet excited state ($\varepsilon_{T1\text{-}Tn}$) and triplet quantum yield (Φ_T) were determined by the partial saturation method.[15] The optical density at the absorption band maximum was monitored when the excitation energy at 355 nm was gradually increased. The following equation was then used to fit the experimental data to obtain the ε_T and Φ_T.[15]

$$\Delta OD = a(1 - \exp(-bI_p)) \quad (2)$$

where ΔOD is the optical density at the corresponding band maximum, I_p is the pump intensity in Einstein.cm^{-2}, $a = (\varepsilon_T - \varepsilon_0)dl$, and $b = 2303\varepsilon_0^{ex}\Phi_T/A$. ε_T and ε_0 are the absorption coefficients of the excited state and the ground state at the band maximum, ε_0^{ex} is the ground-state absorption coefficient at the excitation wavelength of 355 nm, d is the concentration of the sample (mol L^{-1}), l is the thickness of the sample, and A is the area of the sample irradiated by the excitation beam.

Nonlinear Absorption Measurements. The experimental setup was similar to what had been described previously,[16] with a 20 cm lens used to focus the beam to the sample cuvette. The thickness of the cuvette was 2 mm.

Theoretical Calculations. DFT calculations were performed for complexes **6**−**8** and **12** to characterize the highest few occupied and lowest few unoccupied molecular orbitals, and to understand the nature of the low-lying excited states. Additional TDDFT calculations were performed to better characterize the excited states. A hybrid generalized gradient approximation (hybrid GGA) exchange-correlation functional was used for all DFT calculations. The particular hybrid GGA used is known by the acronym MPW3LYP, which consists of the three-parameter modified Perdew−Wang (MPW) exchange functional and the Lee−Yang−Parr (LYP) correlation functional.[17] The basis sets used include functions from the LANL2DZ set[18] and from the 6-31+G** set;[19] the particular combination is abbreviated in this work as LANG6. LANL2DZ is an effective core potential (ECP) basis set and was used to describe the platinum atom; this provides some correction for relativistic effects of the platinum atom. The 6-31+G** basis set was used for descriptions of all other atoms.

Since complex **8** is much larger than complexes **6**, **7**, and **12**, the smaller 6-31G* basis set[19a,b] was used for other atoms except Pt in this complex, while the same LANL2DZ ECP basis set was used for the Pt atom. This combination of basis sets has been abbreviated as LANG631. Full geometry optimizations were performed for complexes **6**−**8** and **12**. Excited singlet electronic states were calculated using the Time-Dependent Density Functional Theory (TDDFT) method[20] with the MPW3LYP exchange-correlation functional. The Gaussian 03 (Rev. C.02) software suite,[21] running on two different computers [SunFire V1280 (OS Solaris 10) and an SGI (OS IRIX64 6.5)], was used to perform all calculations.

Results

Electronic Absorption. The electronic absorption of **6**−**10** in CH_2Cl_2 and CH_3CN obey Beer−Lambert's law in the concentration range of 10^{-6}−10^{-4} mol/L. As depicted in Figure 1, all spectra consist of two groups of electronic transitions. With reference to the reported polypyridine platinum complexes,[1,2a,7−10] the intensive absorption bands in the UV region (<400 nm) are assigned to the intraligand π,π^* transition, while the broad low-energy (400−550 nm) band is tentatively assigned to a charge-transfer transition. The shape and the extinction coefficient of complexes **6**−**8** are quite similar except that **7** and **8** exhibit stronger and broader charge-transfer absorption. As will be discussed later in the discussion section, the broadening of this charge-transfer band could emanate from the mixture of the LLCT

(14) Van Houten, J.; Watts, R. *J. Am. Chem. Soc.* **1976**, *98*, 4853.
(15) Carmichael, I.; Hug, G. L. *J. Phys. Chem. Ref. Data* **1986**, *15*, 1.
(16) Sun, W.; Zhu, H.; Barron, P. M. *Chem. Mater.* **2006**, *18*, 2602.
(17) Zhao, Y.; Truhlar, D. G. *J. Phys. Chem. A* **2004**, *108*, 6908.
(18) (a) Hay, P. J.; Wadt, W. R. *J. Chem. Phys.* **1985**, *82*, 270. (b) Hay, P. J.; Wadt, W. R. *J. Chem. Phys.* **1985**, *82*, 284. (c) Hay, P. J.; Wadt, W. R. *J. Chem. Phys.* **1985**, *82*, 299.
(19) (a) Hariharan, P. C.; Pople, J. A. *Theor. Chim. Acta* **1973**, *28*, 213. (b) Francl, M. M.; Petro, W. J.; Hehre, W. J.; Binkley, J. S.; Gordon, M. S.; DeFrees, D. J.; Pople, J. A. *J. Chem. Phys.* **1982**, *77*, 3654. (c) Clark, T.; Chandrasekhar, J.; Schleyer, P. V. R. *J. Comput. Chem.* **1983**, *4*, 294. (d) Krishnam, R.; Binkley, J. S.; Seeger, R.; Pople, J. A. *J. Chem. Phys.* **1980**, *72*, 650. (e) Gill, P. M. W.; Johnson, B. G.; Pople, J. A.; Frisch, M. J. *Chem. Phys. Lett.* **1992**, *197*, 499.
(20) (a) Stratmann, R. E.; Scuseria, G. E.; Frisch, M. J. *J. Chem. Phys.* **1998**, *109*, 8218. (b) Bauernschmitt, R.; Ahlrichs, R. *Chem. Phys. Lett.* **1996**, *256*, 454. (c) Casida, M. E.; Jamorski, C.; Casida, K. C.; Salahub, D. R. *J. Chem. Phys.* **1998**, *108*, 4439.
(21) Frisch, M. J. et al. *Gaussian 03*, Revision C.02; Gaussian, Inc.: Wallingford, CT, 2004.

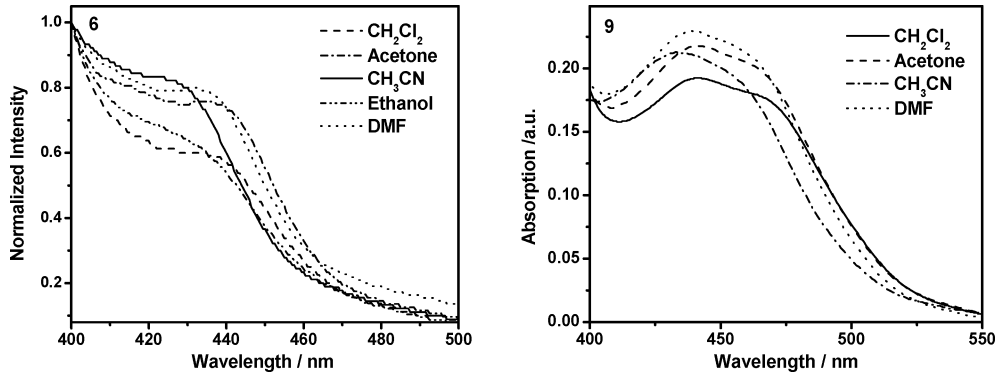

Figure 2. Electronic absorption spectra of **6** and **9** in different solvents.

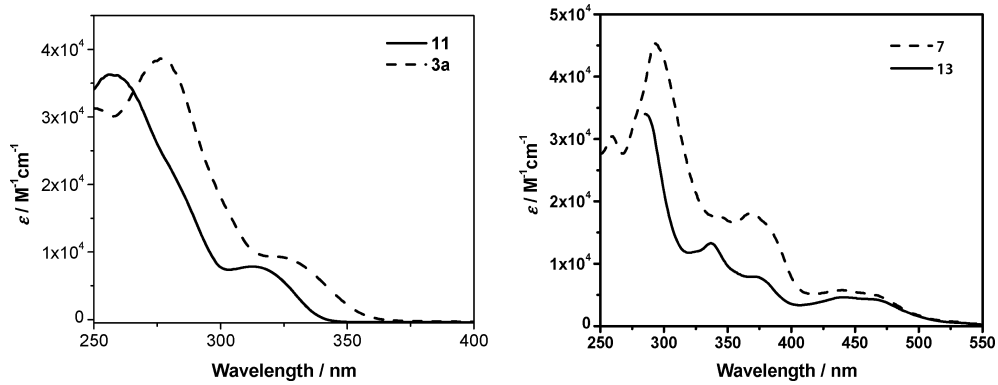

Figure 3. Comparison of the electronic absorption spectra of **3a** and **11**, and **7** and **13** in CH_2Cl_2.

transition into the charge-transfer band. Complex **9**, which possesses a second 4,6-diphenyl-2,2′-bipyridine unit on the ethynyl ligand, has extinction coefficients that almost double those for complex **8** in most wavelengths. From **7** to **9**, the charge-transfer band becomes slightly broader (see inset in Figure 1), and the extinction coefficients gradually increase, which reflects the increased π-donating ability of the ancillary ligand. However, for complex **10** that has the second terdentate ligand coordinated with platinum(II) ion, its electronic absorption spectrum, especially the charge-transfer band, is quite different from that of **9**. Rather than that it almost parallels the spectrum of **6**, except that its extinction coefficients double those of **6** in the UV region, and triple for the charge-transfer transition.

The charge-transfer bands of **6**−**10** exhibit some solvent dependence. As exemplified in Figure 2 for complexes **6** and **9**, the charge-transfer band displays some extent of bathochromic shift in less polar solvents such as CH_2Cl_2 in comparison to that in more polar solvents, such as CH_3CN. This negative solvatochromic effect is also observed in complexes **7**, **8**, and **10** (Supporting Information, Figure S1) and is typical for platinum(II) polypyridine complexes, including the cyclometallated C^N^N platinum complexes reported by Che's group.[2a,7−10]

Another finding from the electronic absorption measurement is the effect of alkoxyl substitution. When comparing the spectrum of the ligand **3a** to that of the "alkoxyl free" ligand **11** (Figure 3), the former exhibits an obvious bathochromic shift with somewhat enhanced intensity. A similar trend was observed in the UV spectral region (<400 nm) of the corresponding platinum complexes, as demonstrated by complexes **7** and **13** in Figure 3. However, the energy of the low-energy charge-transfer band is essentially unaffected by the alkoxyl substitution. The same phenomena have been observed for **6** and **12** (see Supporting Information, Figure S2).

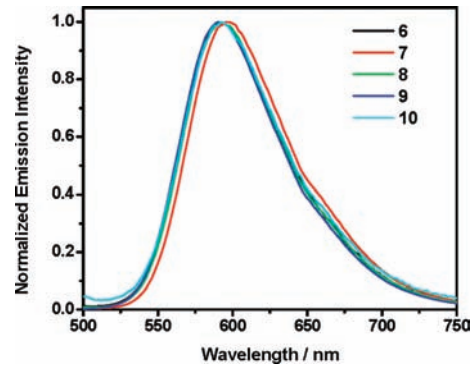

Figure 4. Normalized emission spectra of complexes **6**−**10** in degassed CH_2Cl_2 solutions at room temperature. Excitation was at the charge-transfer band maximum for each complex.

Emission. Complexes **6**−**10** are emissive in fluid solutions at room temperature. In contrast to the influence of the ancillary ligand on the electronic absorption spectra, the effect of these ligands on the emission energy is nominal. As shown in Figure 4 and listed in Table 1, the emission energy of **6** and **8**−**10** appears at about 590 nm. Complex **7** exhibits slightly reduced emission energy at 596 nm in CH_2Cl_2. Except for **6** and **10**, the quantum yields of **7**−**9** are on the order of 15−21% (see Table 1), which is much higher than most of the platinum terdentate complexes reported in the literature,[7−10] and comparable to some of

Table 1. Photophysical Parameters of **6**−**10** at Room Temperature in CH_2Cl_2 and CH_3CN

	CH_2Cl_2			CH_3CN		
	λ_{abs}/nm (ε/M^{-1} cm^{-1})	λ_{em}/nm (τ_{em}/ns; Φ_{em}; $k_r{}^a$ /s^{-1})	$k_q{}^b$/ M^{-1} s^{-1}	λ_{em}/nm (τ_{em}/ns; Φ_{em};$k_r{}^a$ /s^{-1})	$\lambda_{T1\text{-}Tn}$/nm (τ_T/ns; $\varepsilon_{T1\text{-}Tn}{}^c$/$M^{-1}$ cm^{-1})	$\Phi_T{}^d$
6	286 (40800), 300 (43000), 367 (17200), 431 (3840)	590 (740; 0.033; 4.46×10^4)	1.70×10^9	590 (460; 0.006; 1.30×10^4)	400 (310; 10310), 468 (300; 2950), 670	0.27
7	293 (45300), 342 (17600), 368 (18100), 439 (5800), 464 (5040)	596 (670; 0.19; 2.84×10^5)	1.90×10^9	592 (570; 0.035; 6.14×10^4)	400 (500; 8330), 502 (540; 3100), 680, 798	0.34
8	292 (52000), 344 (17800), 366 (19000), 439 (7240), 464 (6570)	590 (980; 0.15; 1.53×10^5)	2.17×10^9	588 (600; 0.032; 5.33×10^4)	405 (660; 8220), 505, 630 (670; 8660), 670	0.42
9	294 (72300), 329 (57100), 441 (11400), 464 (10600)	590 (970; 0.21; 2.16×10^5)	2.01×10^9	588 (660; 0.052; 7.88×10^4)	400 (720; 19730), 495, 650 (750; 2900), 670, 790	0.11
10	286 (59400), 299 (60000), 366 (30100), 436 (11300)	592 (870; 0.008; 9.20×10^3)	2.47×10^9	584 (510; 0.007; 1.37×10^4)	402, 472, 590 (4830; 2650), 656	0.06
12		571 (360; 0.019; 5.28×10^4)		566 (40; 0.001; 2.50×10^4)		
13		596 (400; 0.08; 2.00×10^5)		589 (100; 0.025; 2.50×10^5)	385 (86), 585 (87, 4933)^e	0.51^e

^{a} Radiative decay rate constant ($k_r = \Phi/\tau$). ^{b} Emission self-quenching rate constant. ^{c} The Triplet excited-state absorption coefficient. ^{d} The triplet excited-state formation quantum yield. ^{e} From reference 6f.

the highly emissive diimine platinum(II) bis(acetylide) complexes ($\Phi_{em} = 0.13-0.27$) reported by Eisenberg et al.[22] and Schanze et al.[23] in CH_2Cl_2. In particular, these values are 2−3 times higher than that of the corresponding "alkoxyl free" C^N^N platinum phenylacetylide complex ($\Phi_{em} = 0.07$).[2a] Although the emission efficiency of **6** and **10** is quite distinct from those of **7**−**9**, the lifetimes deduced from the decay of the emission are quite similar for **6**−**10**. They are all on the order of several hundred nanoseconds. Considering such a long lifetime and the drastic Stokes shift of the emission, the emission should originate from a triplet excited state. The lower emission efficiency of **6** and **10** could emanate from the different degrees of mixture of the ^{3}MLCT configuration in the emitting state in comparison to those in **7**−**9**, which is evident from the TDDFT calculations and will be discussed in more details in the discussion section.

Different solvents display a minor effect on the emission energy. Figure 5 depicted the emission spectra of complexes **6** and **9** in different solvents. A similar phenomenon was observed for **7**, **8**, and **10**. Although the solvatochromic effect on the emission energy is insignificant, it is still evident that less polar solvents, such as CH_2Cl_2, cause a slight bathochromic shift of the emission energy compared to polar solvents, such as CH_3CN. This is in line with the charge-transfer transition in the electronic absorption spectra, although the effect is minor. The insensitivity of the emission energy to the polarity of the solvent is in accord with the behavior of the corresponding "alkoxyl free" C^N^N platinum chloride and phenylacetylide complexes reported by Che's group,[2a,9c] but is quite different from the platinum terpyridyl complexes without electron-donating substituent on the terpyridyl ligand reported in literature.[1,7,8a−c,10] Such a disparity suggests that the emitting states for **6**−**10** could be different from the pure ^{3}MLCT state that is commonly assigned for most of the platinum terpyridyl complexes.[1,7,8,10]

The effect of the alkoxyl substitution on emission is noteworthy for complexes **6**, **7** and the ligand **3a** in comparison to their corresponding "alkoxyl free" analogues **12**, **13**, and **11**. As listed in Table 1, the emission energy of **6** in both CH_2Cl_2 and CH_3CN is approximately 20 nm red-shifted with respect to that of **12**. The lifetime of **6** in CH_2Cl_2 doubles that of **12**, while in CH_3CN it is more than 1 order of magnitude longer. The lifetimes of **7** in CH_2Cl_2 and CH_3CN are also much longer than those of **13** in corresponding solvent. In addition, the solvent quenching effect on the lifetime is more drastic for **12** and **13** than for **6** and **7**. Coordinating solvents like CH_3CN reduce the lifetime of **12** and **13** remarkably, that is, approximately 10 times for **12** and 4 times for **13**, while the lifetime reduction for **6** and **7** in CH_3CN is less than one half. For the analogous ligands **3a** and **11**, alkoxyl substitution induces an approximately 30 nm bathochromic shift of the emission energy for **3a**. More significantly, **3a** exhibits a pronounced solvatochromic effect, that is, the emission energy gradually decreases with increased solvent polarity (Figure 6), while **11** shows almost

(22) McGarrah, J. E.; Eisenberg, R. *Inorg. Chem.* **2003**, *42*, 4355.
(23) Whittle, C. E.; Weinstein, J. A.; George, M. W.; Schanze, K. S. *Inorg. Chem.* **2001**, *40*, 4053.

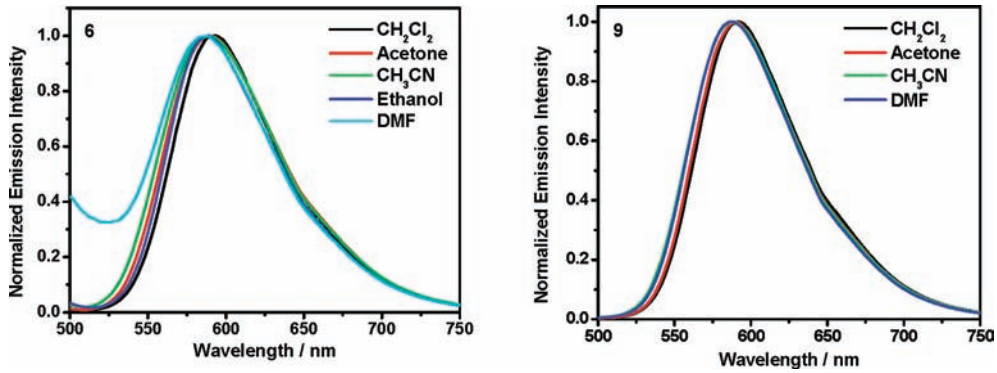

Figure 5. Normalized emission spectra of complexes **6** and **9** in different solvents. The excitation wavelength was 432 nm for **6** and 431 nm for **9**.

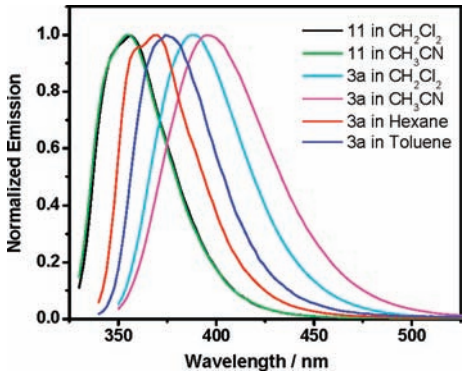

Figure 6. Normalized emission spectra of **3a** and **11** in different solvents.

Table 2. Lifetime of **3a** in Different Solvents at a Concentration of ~1 × 10^{-5} mol/L

solvent	hexane	toluene	CH_2Cl_2	CH_3CN
τ/ns	2.51 ± 0.004	2.76 ± 0.015	2.95 ± 0.015	3.62 ± 0.015

no solvent dependence. In addition, as listed in Table 2, the lifetime of **3a** tended to increase as the polarity of the solvent increased.

The emission energy of **6**−**10** remains constant in the concentration range of 10^{-6} to 10^{-4} mol/L; however, the emission intensity decreases at high concentrations. As exemplified in Figure 7 for complex **9** in CH_2Cl_2, its normalized emission spectrum overlaps very well at various concentrations between 1.1 × 10^{-6} and 2.8 × 10^{-4} mol/L. The emission intensity increases when the concentration increases from 1.1 × 10^{-6} to 5.5 × 10^{-5} mol/L. However, the intensity decreases dramatically when the concentration reaches 2.8 × 10^{-4} mol/L. This phenomenon should be attributed to a self-quenching effect (the quenching of the excited state because of interactions between an excited-state molecule and a ground-state molecule of the same type;[24] in the case of the platinum terdentate complexes, such interactions could result in nonemissive excimers.), which is commonly seen in many organometallic complexes including platinum complexes[9c,10d,25] and is confirmed from the lifetime measurement in different-concentration solutions. The lifetimes of **6**−**10** keep decreasing with increasing concentration. Plotting of the decay rate constant versus complex concentration results in a straight line for each complex (see Supporting Information, Figure S3 for complex **8**). The slope of the straight line corresponds to the self-quenching rate constant (k_q), which is listed in Table 1 and is of the order of 10^9 L mol^{-1} s^{-1} for each complex. These values are in line with those reported for "alkoxyl free" platinum C^N^N complexes (1.6 × 10^9−5.7 × 10^9 L mol^{-1} s^{-1})[2a,9c] and platinum terpyridy phenylacetylide complexes (1.45 × 10^9−1.74 × 10^9 L mol^{-1} s^{-1}).[10f]

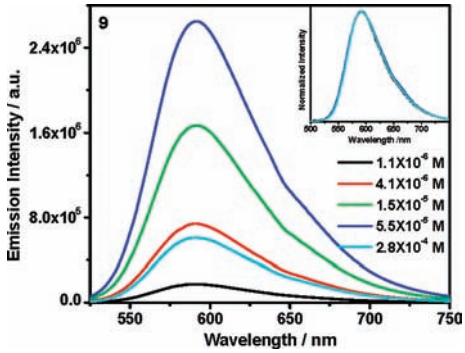

Figure 7. Emission spectra of complex **9** in degassed CH_2Cl_2 solutions at different concentrations at room temperature.

DFT Calculations. TDDFT calculations were carried out on **6**−**8** and **12** to provide insight into the effect of the alkoxyl substitution and explain the ancillary-ligand-independent and solvent-insensitive emission characteristics of **6**−**10**. At the least, the TDDFT calculations are expected to help us to understand the nature of the low-lying excited electronic states.

Figure 8 presents the electron density distribution of the HOMO, HOMO-1, LUMO and LUMO+1 for complex **6**, while similar information is shown in the Supporting Information for complexes **7**, **8**, and **12** (Supporting Information, Figure S4). The relative contributions of each moiety to the corresponding MOs are listed in Table 3. The calculations show that the LUMO is almost exclusively π*(bipyridine) for all complexes. In contrast, the composition of the HOMO is quite different for these complexes. The HOMO is essentially on the 6-phenyl and the central pyridine rings (referred to as C^N component) for complex **6**, with 4.5% contribution from the d(Pt). For complex **7**, the dominant contribution is also from the C^N component, and

(24) Turro, N. J. *Modern Molecular Photochemistry*; University Science Books: Sausalito, CA, 1991; p 357.
(25) (a) Kunkely, H.; Vogler, A. *J. Am. Chem. Soc.* **1990**, *112*, 5625. (b) Wan, K.-T.; Che, C.-M.; Cho, K.-C. *J. Chem. Soc., Dalton Trans.* **1991**, 1077. (c) Hissler, M.; Connick, W. B.; Geiger, D. K.; McGarrah, J. E.; Lipa, D.; Lachicotte, R. J.; Eisenberg, R. *Inorg. Chem.* **2000**, *39*, 447.

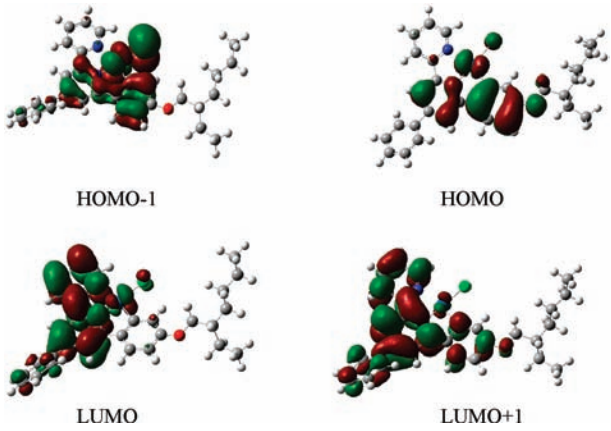

Figure 8. Contour plots of the calculated highest occupied molecular orbital (HOMO), HOMO-1, lowest unoccupied molecular orbital (LUMO) and LUMO+1 for complex **6**.

Table 3. Relative Percent Contribution of Fragments to the MOs in Complexes **6**−**8** and **12**

complex	contribution of fragments (%)	HOMO-1	HOMO	LUMO	LUMO+1
6	Pt	37.7	4.5	0.3	0.0
	Cl	32.0	0.0	0.0	0.0
	C^N	30.3	95.5		
	Bipyridine			99.7	100.0
7	Pt	4.4	15.7	0.4	0.0
	Pr-Acetylide	15.5	19.9	0.5	1.2
	C^N	80.0	64.4		
	Bipyridine			98.8	98.8
8	Pt	29.3	28.8	4.5	0.0
	Ph-Acetylide	5.6	71.2	0.0	0.0
	C^N	65.1	0.0		
	Bipyridine			94.2	100.0
12	Pt	24.8	42.4	0.3	0.2
	Cl	13.4	19.4	0.0	0.0
	C^N	61.9	38.2		
	Bipyridine			99.7	99.8

the d(Pt) and π(C≡C) components contribute 16% and 20%, respectively. However, the HOMO of complex **8** has no contribution from the C^N component; the dominant contribution emanates from the π(C≡CPh) (71%) component and d(Pt) contributes to the remaining 29%. An apparent trend is noted that with the increased π-donating ability of the ancillary ligand, the contribution from the C^N component to the HOMO gradually diminishes, while the contribution from the π(C≡CR) component and the d(Pt) drastically increase. For "alkoxyl free" complex **12**, the π(C^N) and the d(Pt) components contribute almost equally (∼40%) to the HOMO, and the remaining 20% contribution comes from the Cl ligand. The electron-donating alkoxyl substituent apparently increases the contribution of the C^N component to the HOMO in complex **6**.

The excitation energies (eV), wavelengths (nm), oscillator strengths, and dominant contributing configurations obtained at the TDDFT/LANG6 level of theory for complexes **6**, **7**, **8**, and **12** are provided in Table 4 and in the Supporting Information, Table S1, respectively. The calculation results show that electronic transitions with dominant contributing configurations involving the HOMO→LUMO orbital pair occur at 555 nm (1st excited state) for **6**, 578 nm (2nd excited state) for **7**, 637 nm (1st excited state) for **8**, and 534 nm (1st excited state) for **12**. Transitions involving the HOMO→LUMO+1 orbital pair in their dominant configurations appear at 423 nm (5th excited state) for **6**, 454 nm (5th excited state) for **7**, and 463 nm (4th excited state) for **8.** Although the calculated electronic excitation energies (in nm) to the lowest-lying electronic states for **6**−**8** show deviations in the range of 114−173 nm compared to the observed lowest-energy absorption band maxima, the trend is in line with the experimental results. The observed differences between theoretical and experimental results reported in this work are not entirely surprising because the theoretical calculations were performed for compounds in the gas-phase, while the experiments were conducted in solutions. However, information obtained from the electronic structure of the molecules combined with the agreement between theory and experiment in the overall trends of the excitation wavelengths indicates that the TDDFT calculations can be expected to provide additional insight into the nature of the lowest excited states. Such information is useful and aids in the interpretation of the unusual photophysical properties observed in the platinum(II) complexes reported in this paper.

Table 4. Excitation Energies (eV), Wavelengths (nm), Oscillator Strengths, Dominant Contributing Configuration, and the Associated Configuration Coefficient of Five Low-Lying Electronic States of Complex **6** Obtained at the TDDFT/LANG6 Level of Theory

	excitation energy				
S_n	[eV]	[nm]	f	active orbital pair of dominant configuration	configuration coefficient
1	2.23	555	0.0016	HOMO → LUMO	0.66
2	2.52	492	0.0325	HOMO-1 → LUMO	0.65
3	2.56	484	0.0003	HOMO-2 → LUMO	0.67
4	2.66	465	0.0007	HOMO-4 → LUMO	0.67
5	2.93	423	0.0079	HOMO → LUMO+1	0.48

Triplet Transient Difference Absorption. The time-resolved triplet transient difference absorption (TA) spectra of **6**−**9** in CH_3CN are displayed in Figure 9. All the complexes exhibit broad positive absorption from 370 to 820 nm. The spectrum of **10** (Supporting Information, Figure S5) resembles that of **6**, and the spectra of **8** and **9** resemble each other. The TA spectrum of **7** possesses similar features to those of **6**, but with a red-shifted band maximum for the band between 440 and 600 nm and an enhanced absorption in the visible spectral region. Specifically, the peak appears at 468 nm (i.e., 21367 cm^{-1}) for complex **6**, but 502 nm (i.e., 19920 cm^{-1}) for **7**. On the other hand, the bands from 440 to 700 nm become broader and flatter for complexes **8** and **9** in comparison to those for **6**, **7**, and **10**.

In keeping with the charge-transfer absorption energy and the emission energy, the TA absorption energy in the visible spectral region (440−700 nm) is also influenced notably by the alkoxyl substitution. The band maximum of the complexes with an alkoxyl substituent is blue-shifted with respect to those of their corresponding "alkoxyl free" complexes. In particular, the corresponding visible TA band energy decreases from 468 nm (i.e., 21367 cm^{-1}) for **6** to 515 nm (i.e., 19417 cm^{-1}) for **12** in CH_3CN (Supporting Information, Figure S6). For complexes **7** and **13**, the shift appears to be even larger: it is 502 nm (i.e., 19920 cm^{-1}) for **7** but 572 nm (i.e., 17483 cm^{-1}) for **13** in CH_3CN. The similar trend was observed in CH_2Cl_2 solution as exemplified by **7** and **13** in Figure 10. The TA decay lifetimes for **6**−**10** are listed

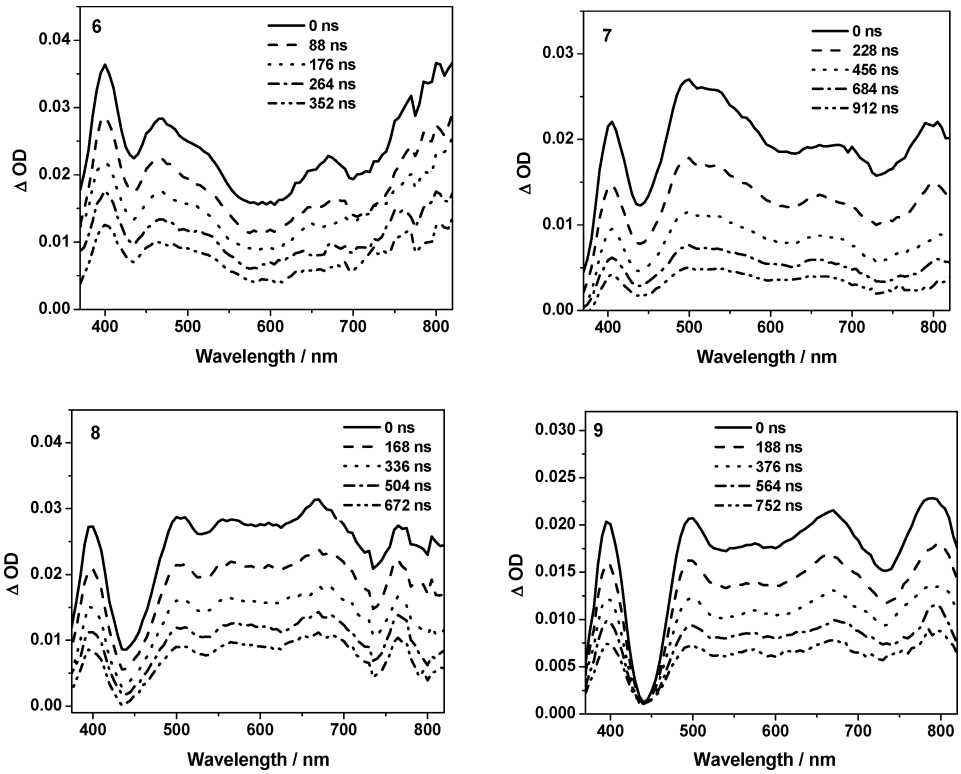

Figure 9. Time-resolved triplet transient difference absorption spectra of complexes **6**−**9** in CH_3CN at room temperature in a 1 cm cuvette. For all complexes, the linear absorptions at 355 nm were adjusted to 0.4. (λ_{ex} = 355 nm).

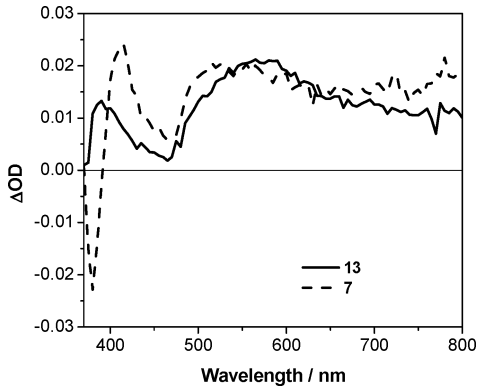

Figure 10. Comparison of the TA spectra of **7** and **13** in CH_2Cl_2 solutions at zero time delay. The linear absorption at 355 nm was adjusted to 0.4 for both samples, and the excitation wavelength was 355 nm.

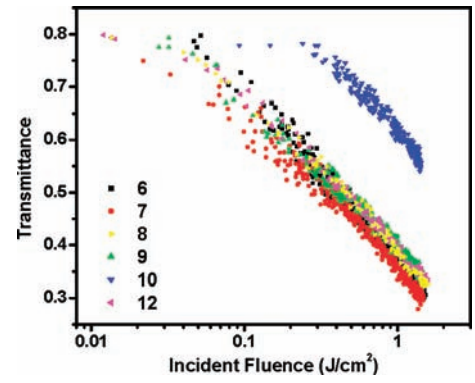

Figure 11. Transmission vs incident fluence curves for **6**−**10** and **12** in CH_2Cl_2 solutions for 4.1 ns laser pulses at 532 nm in a 2 mm cell. The linear transmission was adjusted to 80%.

in Table 1. Except for **10** that exhibits a much longer lifetime, the TA lifetimes of **6**−**9** are all similar to those measured from the decay of emission.

Using the partial saturation method, the triplet excited-state absorption coefficients ($\varepsilon_{T1\text{-}Tn}$) and the quantum yields of triplet excited-state formation (Φ_T) were measured, and the results are given in Table 1. Compounds **6**−**9** show moderate to strong triplet excited-state absorption coefficients at about 400 nm, with $\varepsilon_{T1\text{-}Tn}$ varying from 8.2×10^3 to 2.0×10^4 L mol^{-1} cm^{-1}, while the $\varepsilon_{T1\text{-}Tn}$ for **10** is much smaller. In line with this trend, Φ_T for **10** is quite small, being only 0.06, while the Φ_T's for **6**−**9** are in the range of 0.11−0.42.

Reverse Saturable Absorption. The nonlinear absorption measurements were conducted at 532 nm using nanosecond pulses. Figure 11 shows the results of **6**−**10** and **12** in CH_2Cl_2 solutions. With a linear transmission of 80% in a 2 mm thick quartz cuvette, all complexes exhibit significant transmission decreases with increased incident fluence, which is clearly a characteristic of reverse saturable absorption (RSA). Although the RSA of **6**−**9** and **12** are quite similar, a small difference is still discernible. The degree of RSA follows this trend: **7** ≈ **6** > **8** ≈ **12** ≈ **9** ≫ **10**. The RSA of **6** is clearly stronger than that of its "alkoxyl free" analogue **12**.

Discussion

Nature of the Excited States and the Substituent and Solvent Effects. For the reported platinum terpyridyl complexes,[1,7,10] the ancillary substituent has salient effect on the electronic structure of the complex. The electron densities of the LUMOs of these complexes are essentially localized on the terpyridyl ligand, and those of the HOMOs are dominated by the d(Pt) and the π(C≡CR) components.[10h−j]

Therefore, the lowest singlet excited state is generally regarded as a ^{1}MLCT/^{1}LLCT state, and the emitting state is considered as a ^{3}MLCT state.[1,7,10] As a result, the low-lying ^{1}MLCT/^{1}LLCT transition in the electronic absorption spectrum usually becomes broadened and the ^{3}MLCT emission band is red-shifted when the electron donation ability of the ancillary ligand increases. For example, Yam and co-workers reported that for platinum terpyridyl acetylide complexes with different auxiliary substituents on the phenylacetylide ligand, electron-donating substituents cause bathochromic shifts in their ^{1}MLCT/^{1}LLCT absorption band and ^{3}MLCT emission band, while an electron-withdrawing substituent induces hyposochromic shifts.[10f] Wu and Tung et al. also discovered that in the 4′-tolylterpyridyl platinum(II) acetylide complexes, the complex with the pentynyl ligand possesses a low-energy absorption band at about 441 nm, and the emission appears at 580 nm in CH_2Cl_2.[10g] In contrast, the ^{1}MLCT/^{1}LLCT transition is much broader for the complex with the phenylacetylide ligand, where the band maximum occurs at 433 nm and a shoulder at 482 nm, and the emission is observed at 619 nm.[10g] The similar phenomenon has been observed by Che and co-workers in "alkoxyl free" platinum C^N^N complexes[2a] and by us from complexes **12** and **13**, in which the emission of **12** appears at 566 nm in CH_3CN, but complex **13** emits at about 589 nm.[6f] However, for complexes **6**−**10** studied in this work, the ancillary ligand does not show prominent effect on the low-lying absorption and emission energies. The emission energy of **6**−**10** is essentially the same, and the energy of the low-lying absorption band remains almost the same for **7**−**9**. Moreover, the emission of these complexes did not manifest as significant solvatochromism as the platinum terpyridyl complexes.[1,7,8,10] All these facts imply that the nature of the lowest excited state could be different from the ^{1}MLCT/^{1}LLCT and ^{3}MLCT that are commonly regarded for the platinum terpyridyl complexes. Features that are independent of the acetylide ligand, such as the intraligand π,π^* or ILCT transitions within the C^N^N ligand, must be involved in the lowest excited state.

Che and co-workers have revealed that the emissions of the heteroatom-containing platinum S^N^N and O^N^N complexes are insensitive to the substituent(s) on the arylacetylide ligand, and they tentatively attributed these emissions to the ^{1}ILCT transitions within the S^N^N and O^N^N ligands.[2a] For the platinum 4′-pyrenylterpyridyl chloride complex reported by McMillin et al., the emitting state was considered as an admixture of ^{3}MLCT/^{3}ILCT/$^3\pi,\pi^*$ transitions.[8d] A common feature found in these three systems is that they all contain an electron donating component, that is, thienyl, furyl, and pyrenyl rings, in the terdentate ligand. Considering the electron donating ability of the alkoxyl substituent, we speculate that the transition involved in the lowest excited state is the ILCT transition.

To support this hypothesis, TDDFT calculations were carried out on **6**−**8**. The calculations show that the electron density distribution on the LUMOs of these complexes all have dominant contribution from the π^*(bipyridine), but distributions on the HOMOs of these three complexes have different compositions. For complex **6**, the HOMO is almost exclusively distributed on the C^N component, with 4.5% contribution from the d(Pt). For complex **7**, the majority contribution is still from the C^N component, with the d(Pt) and the π(C≡C) components contributing 16% and 20%, respectively. Conversely, the dominant contribution for complex **8** emanates from the π(C≡CPh) (71%) component and d(Pt) contributes to the remaining 29%, while the C^N component has no contribution. On the basis of the results of these calculations, the nature of the lowest singlet excited state can be assigned tentatively to intraligand-charge-transfer (ILCT, π(C^N) → π^*(bipyridine)) and intraligand π,π^* transitions mixed with a little MLCT (d(Pt) → π^*(bipyridine)) character for complex **6**. For complex **7**, it is a mixture of ILCT, π,π^*, MLCT and LLCT (π(C≡C) → π^*(bipyridine)). For complex **8**, the lowest excited state likely admixes LLCT (π(C≡CPh) → π^*(bipyridine)) and the MLCT characters.

Experimental results coincide with these assignments. First, the involvement of LLCT transition in acetylide containing complexes is manifested by the broadening and the enhancement of the molar extinction coefficients of the low-energy absorption band in complexes **7**−**9** with respect to that of **6**, in which the shoulder of the low-energy absorption band could be mainly attributed to the LLCT. With the increased π-donating ability of the acetylide ligand from **7** to **9**, the relative contribution from the LLCT transition increases. Consequently the relative intensity of the shoulder increases (see the inset plots in Figure 1). In complex **10**, because of the coordination of the second C^N^N ligand with platinum, the electronic density of the C^N^N ligand decreases, which diminishes the contribution from the π[C≡C(C^N^N)] → π^*(bipyridine) LLCT transition. As a result, the profile of the low-energy absorption band in **10** is quite similar to that of **6**. Second, the experimental result that strongly indicates the mixture of MLCT configuration in the lowest singlet excited state is that the low-energy absorption band exhibits negative solvatochromism, which is typical for the charge transfer band in platinum terpyridyl complexes with dominant MLCT character.[1,7,8,10] Third, the involvement of the ILCT and π,π^* transitions in the lowest excited states has been implied by the aforementioned insensitivity of the emissions of **6**−**10** to the nature of the ancillary ligand, and can also be seen from the red-shift and broadening of the low-energy charge-transfer absorption bands and the bathochromic shift of the emissions of **7** and **13** in comparison to those of the corresponding 4′-tolylterpyridyl platinum pentynyl complex.[6f,10g] Other experimental evidence supporting the admixture of the ILCT and π,π^* characters into the lowest excited state includes the minimal solvatochromism of **6**−**10** and the increased excited-state lifetime and reduced solvent quenching effect of **6**, which will be discussed later. Fourthly, the emission quantum yields of **6** and **10** are quite different from those of **7**−**9**. This indicates the different compositions of the emitting excited state, which in turn leads to the different radiative decay rate constants for **6** and **10**.

Resembling most of the platinum polypyridine complexes reported in the literature,[1,7−10] complexes **6**−**10** all emit at

room temperature in fluid solutions, with an emission lifetime of several hundreds of nanoseconds and a Stokes shift of more than 4600 cm^{-1}. Therefore, the emitting state could be attributed to a triplet excited state. However, unlike most of the platinum terpyridyl complexes, the emitting state of **6**−**10** cannot be a pure ^{3}MLCT state because the ^{3}MLCT emission usually exhibits a salient negative solvatochromic effect, and the energy is affected by the electron donating ability of the acetylide ligand, like the cases mentioned earlier for the platinum(II) terpyridyl acetylide complexes.[10g,f] With reference to the character of the singlet excited state, we speculate that the emitting states of **6**−**10** likely admix the ^{3}MLCT, ^{3}ILCT, and $^3\pi,\pi^*$ characters. Experimental evidence that partially supports the notion of admixing ^{3}ILCT configuration into the emitting state arises from the fact that the emission of the ligand **3a** manifests a prominent positive solvatochromic effect (Figure 6). The pronounced solvatochromism of **3a** suggests that the emission is from a charge-transferred state, which can only be intraligand charge transfer in the ligand. Although the emission observed from the ligand is fluorescence in view of its very short lifetime, this result still provides strong implication of the involvement of the ILCT to the emitting state of the complexes. The nominal solvatochromic effect for **6**−**10** could be simply attributed to the delocalization of the electron density in the excited state that is supported by the TDDFT calculation result for the HOMO; or alternatively, to the admixture of configurationally distinct transitions (^{3}MLCT, ^{3}ILCT, and $^3\pi,\pi^*$) into the emitting state. Further support of the mixture of the ILCT configuration into the emitting state comes from the lifetime measurement of these complexes in CH_2Cl_2 and CH_3CN. It is known that CH_3CN is a Lewis base, which can coordinate with the platinum ion. As a result of this coordination, the ^{3}MLCT emission of the platinum complexes usually is quenched, which has been reported in the literature for most of the platinum polypyridyl complexes.[1−10] However, this is not the case for complexes **6**−**10**. Although the lifetimes of **6**−**10** become somewhat shorter in CH_3CN, the reduction is not as drastic as that in the platinum terpyridyl complexes. Considering the independence of the ILCT and π,π^* transitions on the alternation of the metal center, we believe that the emitting state possesses some ILCT and π,π^* characters. The mixture of configurationally distinct transitions, such as ^{3}ILCT, $^3\pi,\pi^*$, and ^{3}MLCT into the emitting state has been proposed by McMillin and co-workers for a 4′-pyrenylterpyridyl platinum chloride complex that contains a strong π-donating pyrenyl substituent; a similar nominal solvent-induced exciplex quenching was observed for this complex in butyronitrile because of the admixture of the ^{3}ILCT and $^3\pi,\pi^*$ configurations in the emitting state.[8d]

The notion of the admixture of configurationally distinct excitations into the emitting state can be used to explain the low emission quantum yields of **6** and **10**. As discussed earlier for the lowest singlet excited states of **6**−**8**, the contribution of MLCT character gradually increases from **6** to **8**. It is reasonable to assume that the triplet emitting states of these complexes have the similar compositions. The increased degree of ^{3}MLCT character in the emitting state of **7** and **8** would increase the radiative decay rate constants (k_r) for these complexes, which in turn increases the emission quantum yields for **7** and **8**. The emitting-state character of **10** is assumed to be similar to that of **6** in view of the similar feature of the electronic absorption spectra of **6** and **10** as discussed earlier. Consequently, the emission quantum yield of **10** is similar to that of **6**.

Effect of the Alkoxyl Substituent. The alkoxyl substituent on the 6-phenyl ring of the C^N^N ligand plays an important role in the electron density distribution and thus on the photophysical properties. Because of the electron-donating ability of the alkoxyl substituent, the electron density of the 6-phenyl ring increases. On the other hand, the bipyridyl component is electron deficient, which would allow for the occurrence of electron transfer from the 6-phenyl component to the bipyridyl component. Our speculation is supported by the TDDFT calculations and several experimental results. The calculation results indicate that for **6**−**8** the LUMOs' electron densities are almost exclusively on the bipyridyl component. For complexes without strong π-donating acetylide ligand, such as **6** and **7**, the HOMO density has predominant contribution from the C^N component. In particular, the HOMO density is essentially all from the C^N component in complex **6**. Comparing the relative contribution from each component to the HOMOs of **6** and **12** (Table 3), it is obvious that the alkoxyl substituent remarkably increases the contribution of the C^N component from ∼38% in **12** to ∼96% in **6**. This in turn increases the ILCT character in the lowest excited states. Consequently, the lifetime of the excited state, particularly the triplet excited state, increases, which is evident by the lifetimes of **6** and **7** with respect to those of **12** and **13** listed in Table 1. Except for the prolonged lifetime of the platinum complexes, the increased charge-transfer character within the C^N^N ligand also leads to an enhanced solvatochromic effect in the ligand, as demonstrated by **3a** in Figure 6. Moreover, the alkoxyl substitution affects the π,π^* transitions of the C^N^N ligand. As exemplified in Figure 3 for ligand **3a** and complex **7** with respect to their "alkoxyl free" analogues **11** and **13**, respectively, alkoxyl substitution causes a bathochromic shift of the absorption bands in the UV region and an increase of the molar extinction coefficients. This reveals that alkoxyl substitution reduces the energy gap but enhances the oscillator strengths of the π,π^* transitions because of the electron donating ability of the alkoxyl substituent and the increased asymmetry of the C^N^N ligand, respectively.

Transient Absorption and RSA. Like many platinum polypyridine acetylide complexes,[2a,4b,6,7a] complexes **6**−**10** exhibit broad and moderately strong triplet transient difference absorption from the near-UV to the near-IR region. Except for complex **10**, the TA lifetimes of complexes **6**−**9** are comparable to those measured from the decay of the emission, indicating that the transient absorption originates from the emitting state or a state that is in equilibrium with the emitting state. Therefore, the transient absorption is tentatively attributed to the ^{3}MLCT/^{3}ILCT/^{3}LLCT state. Although the alkoxyl substituent influences the position of

the maximum of the transient absorption spectra, the overall features of the TA spectra of **6**, **7**, and **8** resemble those of their corresponding "alkoxyl free" analogues (Figure 10 and Supporting Information, Figure S6).[6b,f] However, the auxiliary substituent at the acetylide ligand seems to affect the profile of the transient absorption. In particular, complexes **8** and **9**, which possess π-donating aryl substituents at the acetylide ligand, exhibit a flatter visible absorption band, and the absorption in the visible region for **7** is stronger than that of **6**. These features are likely related to the acetylide ligand. The contribution from the ancillary acetylide ligand cation to the transient absorption of platinum terpyridyl acetylide complexes has been verified by Castellano and coworkers through transient-trapping experiments.[7a] This provides evidence for the notion of the ^{3}LLCT participation in the transient absorption of **7**−**9**. Nevertheless, the broad positive absorption band in the visible to the near-IR region suggests that RSA could occur in this spectral region, which has been verified by the nonlinear absorption measurement at 532 nm (Figure 11).

All mononuclear complexes (**6**−**9**) exhibit significant RSA when the incident fluence increases. The weak RSA of **10** could be ascribed to its large ground-state absorption cross-section (σ_0), which reduces the ratio of the excited-state absorption to ground-state absorption cross-sections (σ_{ex}/σ_0), and the low quantum yield of the triplet excited-state formation. Both of these parameters are found to be critical for RSA of nanosecond laser pulses from our previous studies.[6,16] Disregarding the difference in the triplet excited-state formation quantum yield, the observed trend of the RSA strength for **6**−**10** essentially coincides with their relative ground-state absorption cross-sections at 532 nm, which is 4.2×10^{-19} cm^2 for **6**, 1.6×10^{-18} cm^2 for **7**, 2.4×10^{-18} cm^2 for **8**, 4.0×10^{-18} cm^2 for **9**, and 7.2×10^{-18} cm^2 for **10**. It is worthy of mention that **6** exhibits noticeably stronger RSA than **12** does, which is likely related to the quite different triplet excited-state lifetimes of these two complexes. The excellent RSA of **6** demonstrates another beneficial consequence of the alkoxyl substitution.

Conclusion

The 4,6-diphenyl-2,2′-bipyridine platinum complexes **6**−**10** with alkoxyl substituent on the 6-phenyl ring exhibit enhanced solubility in CH_3CN and CH_2Cl_2. The alkoxyl substituent enriches the electron density of the 6-phenyl ring, leading to the occurrence of the ILCT. TDDFT calculations corroborate the experimental results. Admixture of the ILCT character into the lowest excited states results in enhanced emission, prolonged excited-state lifetime, and reduced solvatochromism and solvent quenching effect. It also contributes to the independence of the emission energies on the ancillary ligand in **6**−**10**. Notably, complexes **7**−**9** show remarkably high emission quantum yields in CH_2Cl_2 ($\Phi_{em} = 0.15-0.21$), which are among the highest values reported in the literature for platinum polypyridine complexes. Not only this, **6**−**10** show broad positive transient absorption from the near-UV to the near-IR region, and exhibit strong RSA at 532 nm for nanosecond laser pulses except for **10**. The studies on the emission energy, lifetime, and RSA clearly demonstrate that, unlike the influence on the platinum terpyridyl complexes, the ancillary acetylide ligand does not influence the triplet excited-state characteristics pronouncedly. Therefore, for future photonic device applications, it would be unnecessary to convert the chloride ligand into acetylide ligand as what is usually required for the platinum terpyridyl chloride complexes. This clearly demonstrates the beneficial consequence of the alkoxyl substitution.

Acknowledgment. Acknowledgment is made to the National Science Foundation (CAREER CHE-0449598 and CHE-0313907) and Army Research Laboratory (W911NF-06-2-0032) for support. We are also grateful to North Dakota State EPSCoR (ND EPSCoR Instrumentation Award) for support.

Supporting Information Available: Normalized electronic absorption spectra of complexes **7** and **8** in different solvents, normalized electronic absorption and emission spectra of **6** and **12** in CH_2Cl_2, plot of k_{obs} versus concentration for complex **8** in CH_2Cl_2, contour plots of the calculated MOs for complexes **7**, **8**, and **12**, time-resolved triplet transient difference absorption spectra of **10** in CH_3CN, comparison of the TA spectra of **6** and **12** in CH_3CN solutions at zero time delay, the excitation energies (eV), wavelengths (nm), oscillator strengths, dominant contributing configuration, and the associated configuration coefficient obtained at the TDDFT/LANG6 level of theory for complexes **7**, **8**, and **12**, and the full author list for ref 21. This material is available free of charge via the Internet at http://pubs.acs.org.

IC801589Q